

Novel vertical image furnace for fast pyrolysis studies

Mélina Christodoulou, Guillaïn Mauviel*, Jacques Lédé, Pascal Beaurain, Mathieu Weber, Hervé Legall & Francis Billaud

LRGP, ENSIC, CNRS-Université de Lorraine, 1 rue Grandville, BP 20451, 54001 Nancy cedex, France.

Abstract : The image furnace is used to mimic experimentally heating conditions representative of a fluidized bed biomass gasifier. The aim of this paper is to demonstrate the feasibility of heat flux density modulation with a new improved vertical image furnace which is based on the former horizontal setup. This is achieved through the comparison of the experimental and theoretical surfaces temperature evolutions. A numerical model is solved in order to estimate the theoretical surface temperature evolution of a char particle immersed in a fluidized bed at 1123K. The goal of the experiments performed with char samples is to reproduce the same temperature evolutions. The surface temperatures profiles are measured by pyrometry in different conditions (constant heat flux density, variation of the heat flux density over time) and compared to the modeling results. The experiments at constant heat flux density show poor agreement with the model, in comparison with experiments made with variable heat flux density. The best agreement is obtained when the heat flux density is decreased from 560 kWm^{-2} to 250 kWm^{-2} in 1 second after a period of 500 ms.

Keywords: image furnace; temperature; pyrometry; fluidized bed; modeling.

1. Introduction

Ligno-cellulosic biomass is nowadays considered as a very promising renewable carbon resource. It represents a relevant alternative to reduce greenhouse gases emissions. During last decades, many scientists and industrials have pointed out its advantages for energy and chemicals production. However its use requires prior processing. Many options are possible such as the thermochemical routes. Pyrolysis is not only a bio-liquid/bio-char production process, but also the first chemical step in any thermal conversion processes like gasification or combustion. The understanding and modeling of these processes require the careful study of this primary pyrolysis step. In this context, this study included in the French GAYA project, led by GDF Suez and funded by ADEME, which aims to produce Synthetic Natural Gas from ligno-cellulosic biomass. GAYA project will develop a demonstration platform for a new biomass gasification and methanation process. The gasification step produces the CO and H_2 mixture which is necessary for the methanation step, which produces bio-methane. In order to up-scale and control this process, the gasification reactor needs to be modelled. An improvement of the thermochemical phenomena knowledge is necessary. These phenomena (pyrolysis, char gasification, tar cracking...) should be characterized through laboratory experiments close to the industrial conditions.

In this context, our objective is to develop a setup which allows studying the primary solid pyrolysis close to the conditions of the fluidized bed gasifier encountered in the GAYA project. More

* To whom correspondence should be addressed. Tel.: +33 (0)3 83 17 52 07. Fax.: +33 (0)3 83 32 29 75. E-mail: guillaïn.mauviel@univ-lorraine.fr

specifically, the biomass particles should have the same spatial and temporal temperature evolutions in the industrial process and in the laboratory experiment. In the case of an industrial reactor, it is not possible to characterize heat transfer conditions between the hot source and the biomass through a single criteria, like hot source temperature or biomass heating rate. In fluidized bed, the heat flux transferred to the biomass by hot bed particles occurs by convection, radiation and conduction. Nevertheless the heat flux density could be simply defined by:

$$\Phi = h\Delta T \quad (1)$$

Since the global heat transfer coefficient h is very high in a fluidized bed (over $200 \text{ W m}^{-2} \text{ K}^{-1}$), the local temperature of biomass increases sharply, stabilizes during pyrolysis [1] and the resulting char finally tends to the bed temperature. The global heat transfer coefficient could be considered constant, but the heat flux density continuously lowers according to the decrease of the temperature difference. In order to reproduce this thermal behaviour, it has been imagined to develop an image furnace since it has the unique ability to provide the very high heat flux densities (more than 100 kW m^{-2}) which are observed in fluidized bed conditions (cf. table 1).

The image furnace is used since a long time for studying chemical reactions but also for simulating solar furnaces. It is based on the principle of focusing the light of a source onto the surface of a solid. First studies started in the 1950's [2]. The image furnaces presented an alternative to solar furnaces which have certain drawbacks like the variability of the available heat flux density according to the sun position and the weather conditions. It enables to heat rapidly and at high temperatures inert solids ($T > 2000 \text{ K}$).

Historically, the carbon arc has been the first type of light source. A great number of configurations were developed, depending for example on the methods for light beams concentration (elliptic or parabolic mirrors, etc). Xenon and mercury-xenon arc lamps were implemented in the 1960s since they were easier to use and more powerful sources [2]. A majority of studies concerned inorganic chemistry (measurements of oxides heat capacities, crystal growth, etc) [2, 3]. In the 1980s, many pioneering works report the use of the image furnace to study biomass thermal degradation (pyrolysis, gasification) [4, 5, 6, 7, 8, 9]. Later on, other works related to pyrolysis studies by means of image furnace have been published [10, 11, 12, 13]. Generally image furnaces provide constant heat flux density [10, 11, 21, 22] since the temperature of the light source is very high (over 4500 K for xenon-arc lamp). This is not compatible with the decreasing heat flux density observed in industrial fluidized bed conditions. Consequently a new type of image furnace should be imagined. In order to evaluate if this new image furnace is able to reproduce the thermal conditions encountered in fluidized beds, the temperature evolution of the sample should be characterized.

In pyrolysis experiments, the temperature measurement is always difficult and questionable [14]. This difficulty is illustrated through a short comparison between different pyrolysis setups. Our comparison is limited to five specific setups: a wire mesh reactor [15, 16], a drop tube reactor [17, 18], a radiant furnace [19, 20] and two image furnaces [10, 11, 12, 21, 22]. The table 1 presents the main technical characteristics of the setups and the type of temperature measurement: thermocouple (TC) or pyrometry.

Table 1. Some operating conditions of different experimental setups.

	Wire mesh reactor [15, 16]	Drop tube reactor [17, 18]	Radiant furnace [19, 20]	Horizontal image furnace		Vertical image furnace
				[10, 11]	[21, 22]	Present study
Principle	Particles lie between two wire meshes. An electrical current pass through meshes which serve as resistance heaters.	Particles are transported at the top of the preheated reactor. They fall with the preheated inert gas.	The sample is suspended in a zone heated by infrared lamps.	Radiation of an arc lamp is concentrated at the surface of a biomass sample.		
				A lens concentrates the radiation	An elliptical mirror concentrates the radiation.	
Kind of biomass samples	Powder	Powder	Biomass pellet	Biomass pellet		Biomass pellet or powder 10 to 500 mg
Mass in reactor	50 mg	250 gh ⁻¹ to 1 kgh ⁻¹	~10 g	~5 g	~300 mg	
Heatingmode Maximal source temperature or heat flux density	Conduction 1400 K	Walls radiation and gas convection 1300K	Radiation(infra red lamps) 28-80 kWm ⁻²	Radiation(xenon-arc lamp)		
				80-130 kWm ⁻²	50-6000 kWm ⁻²	250-560 kWm ⁻²
Sample temperature measurement	Pyrometry TC (K-type)	No	TC	TC (K-type)	Pyrometry	Pyrometry

The parameters used, like the mass sample, the kind of heating, the shape and size of sample (solid or powder) are different according to the apparatus. The wire mesh and free fall use powders whereas the others use massive samples. In the case of pyrolysis, such a feature implies different internal heat transfer limitations: from chemical to heat transfer regime.

Regarding the temperature measurement, Di Blasi et al [19, 20] consider that the thermocouple placed at the centreline of the biomass sample is the reference for the pyrolysis temperature. Grønli & al [10] use thermocouples placed at different positions inside a big cylindrical sample. Hoekstra & al [15, 16] determine the temperature by thermocouple and pyrometry. In their works they measure the wire mesh temperature while it is impossible to determine the sample temperature. For Zanzi & al [18, 19], the reference temperature is the temperature of the electrical heaters of the reactor as the gases introduced are preheated at the same temperature. In the present study with the image furnace, the surface temperature of the sample is measured by pyrometry. In conclusion, it can be observed that the temperature reference varies significantly between the setups.

Lédé [1, 14] and Narayan & Antal [29] showed that, in the case of biomass pyrolysis, there is a temperature stabilization phenomenon due to thermochemical reaction. The result is that a thermal lag exists between the heat source and the sample temperature. Hoekstra & al [15, 16, 17] take into account the lag in temperature between the mesh and the biomass sample. They calculated an

indication of the reduction of average heating rate of the sample due to heat transfer resistance. Finally, it appears that a direct measurement of the sample temperature is necessary but hard to achieve in fast pyrolysis conditions, since the spatial temperature gradients are high and the temperature evolution is rapid. Accurate measurements with thermocouples (TC) seem difficult. Indeed good contact between pyrolysing biomass and the thermocouple itself should be achieved in order to be sure that the thermocouple temperature is the same as that of sample. However contact thermal resistances exist between the two interfaces. Besides the exact position of the thermocouple can be defined at $\pm 0,1$ mm which may not be accurate enough in fast pyrolysis conditions. Conversely, pyrometry is non-invasive and sufficiently fast, but is restricted to surface. Attention should be paid to the light reflection over the sample which could blur the pyrometer.

The present paper reports first results obtained with a new image furnace operating with variable heat flux density. [The pyrometry measurements allow verifying if the experimental thermal conditions are close to the fluidized bed thermal conditions.](#)

2. Material and methods

2.1. *Image furnace: the former horizontal setup*

The new vertical image furnace relies on the basis of the experimental setup used earlier in our laboratory, which has been described in details in previous papers [12, 13, 23, 24, 25]. The basic principle of this former horizontal setup is to concentrate the radiation of a light source thanks to an elliptical mirror. The light beams are concentrated on a biomass sample, which is placed inside a cylindrical transparent quartz reactor swept by cool nitrogen. The advantages of this former setup are the followings:

- It is dedicated to selectively study primary solids reactions.
- Indeed, there are no secondary reactions in the gas phase because cool nitrogen flows through the quartz reactor.
- The radiation is applied at a specific point of the sample.
- The nitrogen does not absorb the lamp radiation conversely to the solid.
- The experiments are performed with thick samples (few millimetres thickness).
- The sample exposure time to the heat source is measured.
- The mass of all products is measured, which allows to achieve mass balances.

The drawbacks are:

- The samples must be thick in order to be self-supporting; experiment with fluid or powder samples are not possible.
- The applied heat flux density is constant during one experiment.
- [It is not possible to measure surface temperature and recover volatile products during the same experiment.](#)
- The optical properties of the biomass must be known to adjust a model to the experiments.
- [The sample surface is small \(the diameter equals 10 mm\). This surface is limited by the space distribution of the radiation; it follows a Gaussian distribution \[22\]. At the focal point, the heat flux density can be considered uniformly over ten millimetres.](#)

2.2. The vertical image furnace apparatus

The novel vertical image furnace is based on the former horizontal setup. The light source is still an air cooled 5000 W xenon high pressure arc lamp (Osram XBO 5000 W/H CL OFR). This lamp is settled at the first focus of an elliptical mirror (cf. fig.1). The light beams are concentrated at the second focus, where is placed the sample inside a cylindrical reactor.

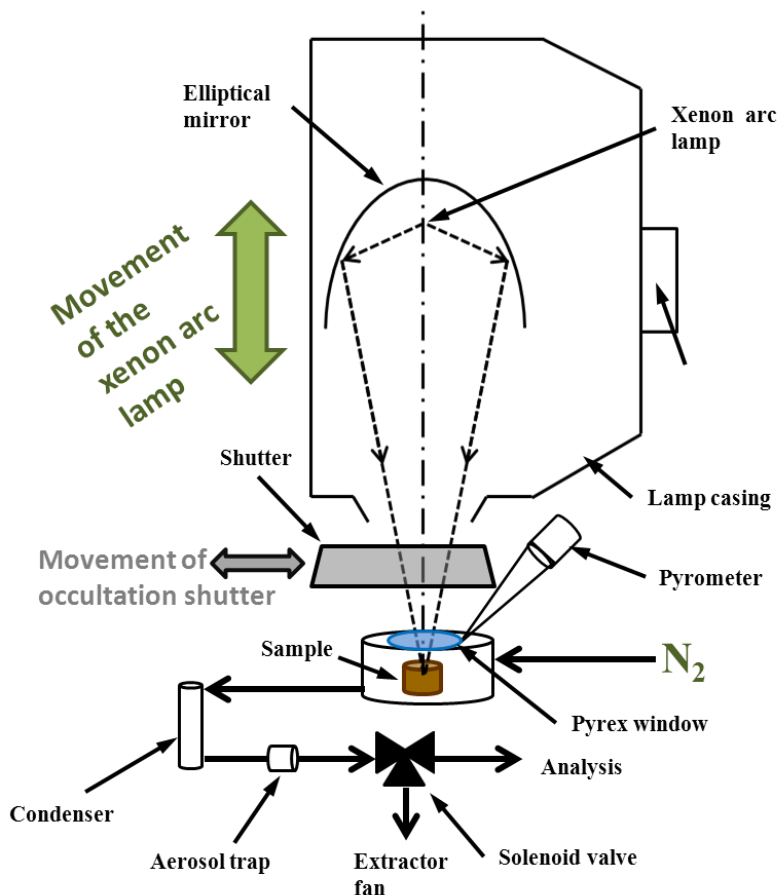


Figure1. Scheme of the vertical image furnace.

The vertical image furnace underwent several modifications in order to overcome some of the disadvantages of the former horizontal setup. It allows working with very thin layer since the sample is horizontal. It can be fine particles or a fluid. An originality of this vertical setup is its ability to tune the heat flux density applied to the sample as a function of time in order to reproduce the heat transfer conditions encountered in a thermo-chemical reactor. The light radiation is maximum when the sample is placed at the second focus of the elliptical mirror. When the sample is moved away from this second focus, the applied heat flux density decreases. It has been chosen to displace the lamp instead of the sample. This feature would allow weighing directly the sample in future experiments. The lamp movement system is controlled by a computer, which allows imposing the lamp initial and final positions, as well as the motion speed of the lamp casing. The maximal travel distance of the lamp casing is 100 mm; the accuracy of the position is about 0.1 mm. The maximum speed to move up is 18 mm s^{-1} , and the maximum speed to move down is 65 mm s^{-1} .

A power sensor (Ophir thermal Head 1000W) is used to measure the heat flux density according to the lamp position. The power sensor measures the available flux P . The window diameter D_w used for

the sensor equals 4 mm. Given this diameter and the measured power, it is possible to compute the heat flux density available by the equation 2.

$$\Phi = 4P / (\pi D_w^2) \quad (2)$$

The flash times are controlled by an occultation shutter. A ceramic plate is fixed on a pneumatic track (Parker Origa, P210/20-32-500). In off position, the ceramic plate intercepts the light beams. During experiment, an exposure time is imposed by computer. The travelling time of the shutter is equal to 300 ms. The shorter value of the flash time is 1 s with an accuracy of 10 ms.

2.3. Pyrolysis reactor

The reactor is made up of two parts, shown in figure 2. The first part is a stainless steel cylinder (inside diameter, 5.5×10^{-2} m; height, 5×10^{-2} m), including a Pyrex window (inside diameter, 3.5×10^{-2} m; height, 3.3×10^{-3} m) at its top. The second part is the air cooling jacket for the pyrometer, which is also swept by nitrogen and connected by a pipe to the top of the reaction chamber. There is an other sweep gas inlet under the Pyrex window. The flow rates of these sweep gases are controlled by mass flow meters (Brook Instruments 5850 S and 5850 TR, total flow $3 \times 10^{-5} \text{ m}^3 \text{ s}^{-1}$ [STP]). The sample is placed at the center of the first part. It is generally positioned at the second focus of the elliptical mirror through the use of two laser beams. The temperature of the sample surface is measured by pyrometry. The pyrometer Impac IN 5H plus cannot measure temperatures over 1183K. Its wavelengths range is between 8 and 14 μm . At this range, the char emissivity is 94% and the pyrometer measurement is not blurred by the image furnace light reflection (0.2 to 1.6 μm). The response time of the pyrometer is about 20 ms.

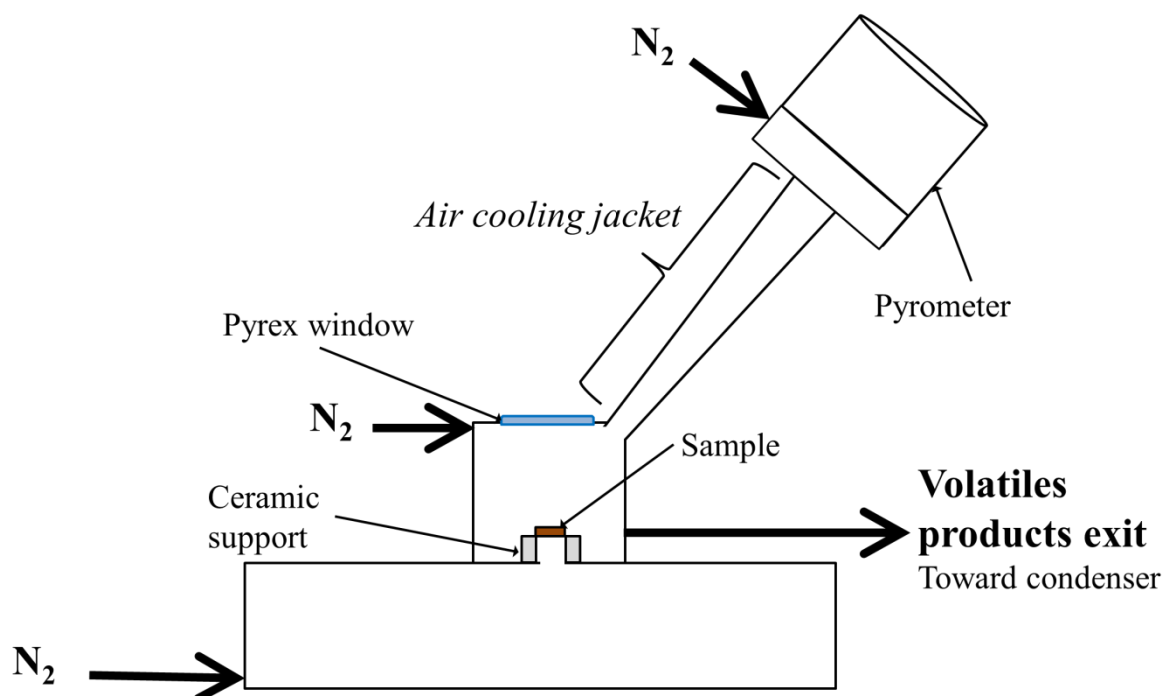


Figure2. Scheme of the reactor.

2.4. Sample

The samples are char particles, which are prepared in preliminary experiments i.e. wood samples pyrolysis in the image furnace at 560 kWm^{-2} . The heating time is 1 min to assure the total conversion of wood in char. The initial wood pellets are 10 mm width and 3 mm thick. The obtained char pellets are 10 mm width and 2 mm thick ($\pm 0.1 \text{ mm}$). The experimental data presented in this paper are measured on these char samples since the goal of this paper is to demonstrate the feasibility of heat flux density modulation with the image furnace. Since the study is limited to char samples, it allows avoiding taking pyrolytic reactions into account in the model. Furthermore, it was simpler for a first approach to achieve measurements on non-reactive samples like char particles since there is no tar aerosols emissions in this case. These thick char samples are laid down on a ceramic support designed to minimize contact surface between sample and support. Thus the conductive heat losses are negligible.

3. Theoretical model

In fluidized bed, the heat flux transferred to the samples occurs by convection, radiation and conduction. A simple thermal modeling is used in order to determine the theoretical temperature evolution of a flat char particle immersed in a fluidized bed. The heat transfer is represented by a simple convection equation (Eq. 1) and uses global heat transfer coefficient h . Typically, this coefficient varies between 200 and $1000 \text{ Wm}^{-2}\text{K}^{-1}$ in fluidized beds [25, 26, 27, 28]. It is intended to compare the experimental surface temperature evolution of char with the theoretical evolution which would be encountered in a fluidized bed gasifier (bed temperature $T_r = 1123 \text{ K}$). The global heat transfer coefficient is assumed to be constant and equal to $500 \text{ Wm}^{-2}\text{K}^{-1}$. Other numerical data are reported in table 2. The cylindrical particle receives the heat flux density in the tangential direction of the wood fibres; the “x” axis is along this direction.

The energy conservation is represented in equation 3.

$$\rho C_p \frac{\partial T}{\partial t} = \lambda \frac{(\partial^2 T)}{(\partial x^2)} \quad (3)$$

The initial condition is the ambient temperature uniformity (equation 4).

$$T_{(x,t=0)} = T_0 \quad (4)$$

For the middle of the char particle ($x = 0$), the symmetry boundary condition is applied (equation 5).

$$\left(\frac{\partial T}{\partial x} \right)_{(x=0,t)} = 0 \quad (5)$$

At the surface ($x=L$), the boundary condition is the heat flux density conservation (equation 6).

$$\lambda \left(\frac{\partial T}{\partial x} \right)_{(x=L,t)} = -h(T - T_r) \quad (6)$$

The partial differential equation (3) is solved by the methods of lines with the Adams-Bashforth-Moulton solver.

Table 2. Values of conditions and physicochemical parameters used to solve the model

Parameters	Values	References
Cp	$420 + 2,09 T - 6,85 \cdot 10^{-4} T^2$	[12]
ρ	170	[21]
λ	0.10	[12]
L	2×10^{-3}	measured
h	500	estimated
T_r	1123	
T_0	300	estimated

4. Results & Discussion

4.1. Heat flux density according to the lamp position

The figure3 represents the heat flux densities measured according to the lamp position. At zero, the heat flux density is the lowest (250 kWm^{-2}). At 65 mm, the heat flux density is maximal (560 kWm^{-2}): in this case, the sample is at the second focus of the elliptical mirror. In a fluidized bed reactor operating at 1123 K, the initial heat flux density imposed on the sample surface ranges between 160 and 800 kWm^{-2} . It is in relatively good agreement with the heat flux densities obtained in the experimental setup. Besides, the vertical image furnace enables to vary the heat flux density applied to the sample. Thus it can be decreased over time in order to reproduce the heat flux density undergone by a particle inside a fluidized bed.

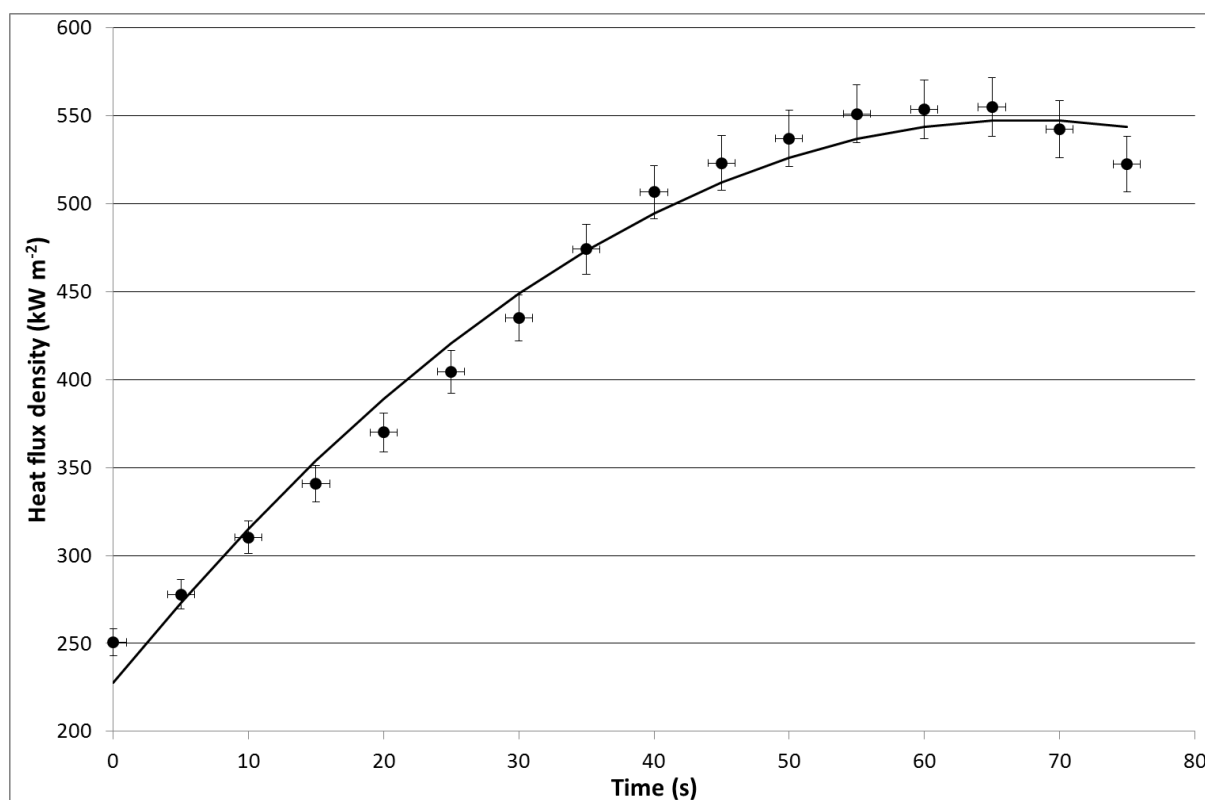


Figure 3. Heat flux density according to the lamp position.

4.2. Results

Figure 4 shows the surface temperature vs. time evolution for different experimental conditions. At constant heat flux density, the lamp does not move and stay at a given position, 65mm for a heat flux density equals to 560 kWm^{-2} and 0mm for 250 kWm^{-2} .

The two experiments, performed at 560 kWm^{-2} are carried out after an interval of 2 months with char sample prepared in same conditions. Their surface temperature profiles are similar showing good repeatability of the measurements. The final temperature exceeds the pyrometer limit ($T_{\text{max}} = 1183\text{K}$). The surface temperature obtained at 560 kWm^{-2} increases less rapidly than the model temperature, but the final temperature largely exceeds the temperature of the fluidized bed reactor ($T_r = 1123\text{K}$).

At 250 kWm^{-2} , the lowest available heat flux density, the surface temperature increases slowly in comparison with the model temperature, but they tend to have similar final value.

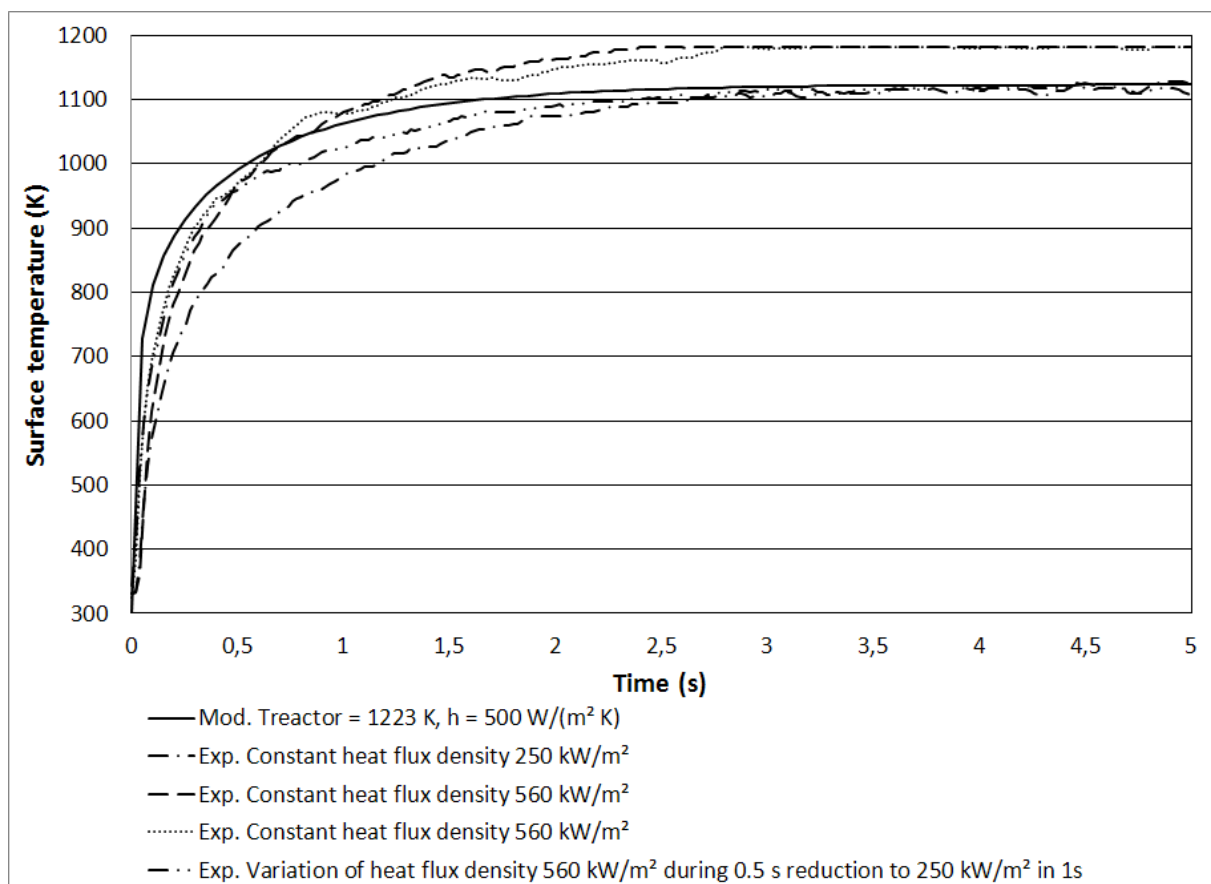


Figure4. Temperature profiles at the surface of wood char at constant heat flux density and at variable heat flux density. Comparison with the model.

With variable heat flux density, different conditions have been explored. Before the start, the image furnace is systematically placed where the heat flux is maximal. The char sample is exposed at this flux during a fixed period, and then the heat flux decreases up to the lower heat flux in 1 s. It can be observed on figure 4 that the temperature rise is fast. When the heat flux density is reduced after a fixed period of 0.5 s, the temperature profile tends toward the temperature evolution at 250 kWm^{-2} : after 3 s, it is in accordance with this curve. These conditions were the best to reproduce the model temperature. Other experiments were done where the maximum heat flux density was maintained

during 1 or 2 seconds. They are not shown on figure 4. These conditions were less realistic because the surface temperature went through a maximum.

For short times, the experimental temperature is systematically lower than the model temperature: the difference is about 200K after 0.1 s, and 130 K near 0.2 s. Above 0.7 s, this difference tends to reverse, but it has been shown that it is possible to make these temperatures converge thanks to the heat flux density reduction.

As a consequence, the maximum heat flux density of the image furnace should be raised to have a better agreement between the experiments and the modeling in the first 500 milliseconds.

4.3. Discussion

The experiments are carried out with char samples in order to demonstrate that it is now possible to alter the heat flux density according to the exposure time. One of our main results is that the variation of the heat flux density enables to tend toward the modeling curve. This modification is relevant and judicious for reproducing fluidized bed reactor conditions. However, the surface temperature evolution measured shows that the heat flux density applied during the first 500ms is not high enough. The difference between the modeling and experimental surface temperatures is higher than 100K from 50 ms to 250 ms. Considering that for very thin sample (near the chemical regime) the pyrolysis lasts around 1s, it will be a critical point to increase the maximum heat flux density.

The preliminary temperature measurements have been made on char in order to avoid the potential problems due to tar aerosols produced by biomass pyrolysis. These aerosols could possibly mask the biomass surface and disturb the pyrometric measurements. In addition, the char has the advantage to undergo no chemical reactions which could infer a complex temperature stabilization phenomenon [1, 14, 29]. The number of assumptions on physico-chemical parameters is also reduced.

Further experiments will be made with biomass samples. In that case, and with the same heat flux densities profiles, the surface temperature evolution of biomass sample will be different because of the reflectivity differences and the chemical reactions. The aerosol masking effect will be managed thanks to the nitrogen sweep gas.

5. Conclusion

The new vertical image furnace has the main objective to reproduce the heat transfer conditions of fluidized bed gasifier. The comparison with other pyrolysis setups shows the difficulty of the sample temperature measurement in fast pyrolysis conditions. It is important to remind that it is not possible to consider that the temperature of the sample is the same as the temperature of the heat source (thermal lag effect). The pyrometric temperature measurement seems to be accurate if some limitations are taken into considerations : light reflection which could blur the pyrometer, emissivity determination, and restriction to surface temperature measurement.

Regarding the heat transfer conditions, the variation of the heat flux density enables to be in better agreement with the fluidized bed model than the configuration with a constant heat flux density. In this first approach, the vertical image furnace appears to be a good experimental setup to simulate fluidized bed conditions. Some modifications, like the raise of the maximum heat flux density, must be done to have a better accordance.

Our final objective is to improve the knowledge of the pyrolysis phenomenon in fluidized bed conditions. The next experiments will be performed on biomass samples. The study will also include the measurement of the temperature evolution of the exposed and unexposed surfaces of thick samples: this will bring interesting experimental data to be compared with theoretical model.

Acknowledgements

The research has been performed thanks to the French Environment and Energy Management Agency (ADEME) financial support through the GAYA Project led by GDF SUEZ.

Nomenclature

D	Diameter (m)
C_p	Sample heat capacity ($J\ kg^{-1}\ K^{-1}$)
H	Global heat transfer coefficient between the bed and the particle sample ($Wm^{-2}K^{-1}$)
L	Characteristic length (m), i.e. thickness of the biomass sample in the image furnace experiments or half-thickness of the cylindrical pellet immersed in a fluidized bed gasifier.
t	Time (s)
T	Temperature (K)
ΔT	Temperature difference between the fluidized bed and the particle sample surface (K).
P	Power measured (W)
x	Axis in the tangential direction of wood fibres (m)

Greek symbols

Φ	Available heat flux density (Wm^{-2})
λ	Sample thermal conductivity ($Wm^{-1}K^{-1}$)
ρ	Sample density (kgm^{-3})
σ	Stefan-Boltzmann constant, 5.67×10^{-8} ($Wm^{-2}K^{-4}$)

Subscripts

r	reactor
0	initial
w	window of the power sensor

Bibliography

- [1] J. L    , Biomass Pyrolysis: Comments on Some Sources of Confusions in the Definitions of Temperatures and Heating Rates, *Energies*, (2010) 886-98.
- [2] P. E. Glaser, R. F. Walker, Thermal imaging techniques: Proceedings of a conference, Arthur D. Little, Cambridge, MA, 1962.
- [3] S. B. Martin, Diffusion-controlled ignition of cellulosic materials by intense radiant energy, *Symposium International on Combustion*. (1965) 877-896.
- [4] J. L    , P. Berthelot, J. Villermaux, A. Rolin, H. Fran  ois, X. Deglise, « Pyrolyse-flash de d  chets ligno-cellulosiques en vue de leur valorisation par l  nergie solaire concentr  e », *Revue de Physique Appliqu  e*, 15 (1980) 545-552.

- [5] S. Caubet, P. Corte, C. Fahim, J. P. Traverse. Thermochemical conversion of biomass: Gasification by flash pyrolysis study, *Sol. Energy*, 29 (1982) 565-572.
- [6] W. C. Chan, M. Kelbon, B. B. Krieger, Modelling and experimental verification of physical and chemical processes during pyrolysis of a large biomass particle, *Fuel*, 64 (1985) 1505-1513.
- [7] M.J. Antal, L. Hofmann, J. Moreira, CT Brown, R. Steenblik, Design and operation of a solar fired biomass flash pyrolysis reactor, *Sol. Energy*, 30 (1983) 299-312.
- [8] M. W. Hopkins, C. DeJenga, M. J. Antal Jr., The flash pyrolysis of cellulosic materials using concentrated visible light, *Sol. Energy*, v 32 (1984) 547-551.
- [9] Tabatabaie-Raissi and M. J. Antal Jr., Design and operation of a 30KWe/2KWth downward facing beam ARC image furnace, *Sol. Energy*, 36 (1986) 419-429.
- [10] M. G. Grønli, M. C. Melaaen, Mathematical Model for Wood Pyrolysis Comparison of Experimental Measurements with Model Predictions, *Energ. Fuel*, 14 (2000) 791-800.
- [11] M. G. Grønli, Thesis of the Norwegian University of Science and Technology, Faculty of Mechanical Engineering, 1996.
- [12] O. Boutin, M. Ferrer, J. Lédé, Flash pyrolysis of cellulose pellets submitted to a concentrated radiation: Experiments and modelling, *Chem. Eng. Sci.*, 57 (2002) 15-25.
- [13] O. Boutin, Thèse de l'Institut National Polytechnique, CRNS-Nancy Université, 1999.
- [14] J. Lédé, O. Authier, Characterization of biomass fast pyrolysis, *Biomass Conv. Bioref.*, 1 (2011) 133-147.
- [15] E. Hoekstra, W.P.M. Van Swaaij, S.R.A. Kersten, J.A. Hogendoorn, Fast pyrolysis in a novel wire-mesh reactor: initial decomposition products of pine wood. *Chem. Eng. J.*, 187 (2012) 172-184.
- [16] E. Hoekstra, Thesis of University of Twente, Thermo-Chemical Conversion of Biomass, 1996.
- [17] R. Zanzi, K. Sjöström, E. Björnbom, Rapid high-temperature pyrolysis of biomass in a free-fall reactor, *Fuel*, 75 (1996) 545-550.
- [18] R. Zanzi, K. Sjöström, E. Björnbom, Rapid pyrolysis of agricultural residues at high temperature, *Biomass and Bioenerg.*, 23 (2002) 357-366.
- [19] C. Di Blasi, C. Branca, A. Santoro, E. Gonzalez Hernandez, Pyrolytic behavior and products of some wood varieties, *Combust. Flame*, 124 (2001) 165-177.
- [20] C. Di Blasi, C. Branca, A. Santoro, R. A. Perez Bermudez, Weight loss dynamics of wood chips under fast radiative heating, *J. Anal. Appl. Pyrol.*, 57 (2001) 77-90.
- [21] O. Authier, M. Ferrer, G. Mauviel, A.-E. Khalfi, J. Lede, Wood Fast Pyrolysis: Comparison of Lagrangian and Eulerian Modeling Approaches with Experimental Measurements, *Ind. Eng. Chem. Res.*, 48 (2009) 4796-4809.
- [22] O. Authier, Thèse de l'Institut National Polytechnique, CRNS-Nancy Université, 2010.
- [23] M. Auber, Thèse de l'Institut National Polytechnique, CRNS-Nancy Université, 2009.
- [24] S. Kohler, Thèse de l'Institut National Polytechnique, CRNS-Nancy Université, 2009.
- [25] P. K. Agarwal, Transport phenomena in multi-particle systems—IV. Heat transfer to a large freely moving particle in gas fluidized bed of smaller particles, *Chem. Eng. Sci.*, 46 (1991) 1115-1127.
- [26] Dyrness, L. R. Glicksman, T. Yule, Heat transfer in the splash zone of a bubbling fluidized bed, *Int. J. Heat and Mass Tran.*, 35 (1992) 847-860.
- [27] C. Di Blasi, C. Branca, Temperatures of Wood Particles in a Hot Sand Bed Fluidized by Nitrogen, *Energ. Fuel*, 17 (2002) 247-254.
- [28] S.N. Oka, Fluidized bed combustion Chapter3. Heat and mass transfer in fluidized beds, Marcel Dekker, E.J. Anthony, New York, (2004).

- [29] R. Narayan, M. J. Antal, Thermal Lag, Fusion, and the Compensation Effect during Biomass Pyrolysis, *Ind. Eng. Chem. Res.*, 35 (1996) 1711-1721.